

MiRNA-20a promotes osteogenic differentiation of human mesenchymal stem cells by co-regulating BMP signaling

Jin-fang Zhang,^{1,2} Wei-ming Fu,³ Ming-liang He,^{3,6} Wei-dong Xie,² Qing Lv,^{1,2} Gang Wan,^{1,2} Guo Li,³ Hua Wang,³ Gang Lu,⁵ Xiang Hu,⁴ Su Jiang,⁴ Jian-na Li,² Marie C.M. Lin,⁵ Ya-ou Zhang^{2,*} and Hsiang-fu Kung^{3,6,7,*}

¹School of life sciences; Tsinghua University; Beijing; ²Life Science Division; Graduate School at Shenzhen; Tsinghua University; Shenzhen;

³Stanley Ho Centre for Emerging Infectious Diseases; The Chinese University of Hong Kong; Hong Kong; ⁴R&D Center of Stem Cell; Engineering and Technology; Shenzhen;

⁵Brain Tumor Center; Neurosurgery; Faculty of Medicine; The Chinese University of Hong Kong; Prince of Wales Hospital; Shatin; ⁶i Ka Shing Institute of Health Sciences; the Chinese University of Hong Kong; Hong Kong; ⁷State Key Laboratory of Oncology in South China; Cancer Center; Sun Yat-Sen University; Guangzhou, China

Key words: mesenchymal stem cell, miR-20a, osteogenic differentiation, BMP signaling pathway, co-regulatory pattern

Abbreviations: hMSC, human mesenchymal stem cells; miR-20a, microRNA-20a; α -MEM, minimum essential medium, alpha medium; BM, bone marrow; GAPDH, glyceraldehyde-3-phosphate dehydrogenase; GFP, green fluorescence protein; siRNA, small interfering ribonucleic acid; BMP2/4, bone morphogenetic protein 2/4; Runx2, runt-related transcription factor 2; PPAR γ , peroxisome-proliferator-activated receptor; AKP, alkaline phosphatase; OPN, osteopontin; OCN, osteocalcin; ARS, alizarin red staining; Osx, osterix

Osteogenic differentiation of mesenchymal stem cells (MSCs) is a complex process, which is regulated by various factors including microRNAs. Our preliminary data showed that the expression of endogenous miR-20a was increased during the course of osteogenic differentiation. Simultaneously, the expression of osteoblast markers and regulators BMP2, BMP4, Runx2, Osx, OCN and OPN was also elevated whereas adipocyte markers PPAR γ and osteoblast antagonist, Bambi and Crim1, were downregulated, thereby suggesting that miR-20a plays an important role in regulating osteoblast differentiation. To validate this hypothesis, we tested its effects on osteogenic differentiation by introducing miR-20a mimics and lentiviral-miR20a-expression vectors into hMSCs. We showed that miR-20a promoted osteogenic differentiation by the upregulation of BMP/Runx2 signaling. We performed bioinformatics analysis and predicted that PPAR γ , Bambi and Crim1 would be potential targets of miR-20a. PPAR γ is a negative regulator of BMP/Runx2 signaling whereas Bambi or Crim1 are antagonists of the BMP pathway. Furthermore, we confirmed that all these molecules were indeed the targets of miR-20a by luciferase reporter, quantitative RT-PCR and western blot assays. Similarly to miR-20a overexpression, the osteogenesis was enhanced by the silence of PPAR γ , Bambi or Crim1 by specific siRNAs. Taken together, for the first time, we demonstrated that miR-20a promoted the osteogenesis of hMSCs in a co-regulatory pattern by targeting PPAR γ , Bambi and Crim1, the negative regulators of BMP signaling.

Introduction

Human mesenchymal stem cells (hMSCs) are multipotent cells which can differentiate into various cells including adipocytes, osteoblasts and chondrocytes.¹ The major factors defining the MSCs' lineage include Runx2 (osteogenic), PPAR γ (adipogenic) and Sox9 (chondrogenic).²⁻⁴ These protein factors, together with several signaling pathways, regulate the MSCs' differentiation towards different lineages. BMPs/Runx2 signaling plays a crucial role in the osteogenesis of the MSCs whereas the PPAR γ activated by C/EBPs stimulates adipogenesis.^{5,6}

MiRNAs are a family of small non-coding RNAs, which have been shown to be responsible for diverse features in animals.⁷ Mature miRNAs are 18–24 nucleotides in length. MiRNA is

generated by an RNase III-type enzyme from an endogenous transcript that contains a local hairpin structure. Being a novel class of gene regulators, miRNAs have attracted great attention. They silence gene expression post-transcriptionally by base pairing to the 3' untranslated regions of target miRNAs, thus resulting in translational repression or RNA cleavage.⁸ It is well known that miRNAs play pivotal roles in various biological processes, including the cell fate choices of embryonic stem cells, cell proliferation, apoptosis, differentiation, morphogenesis, carcinogenesis and angiogenesis.⁹⁻¹² MiRNAs, such as miR-26a, miR-29b, miR-125b, miR-133, miR-135 and miR-196a, have been reported to be involved in osteogenesis by targeting BMP signaling molecules, anti-osteogenic factors and/or bone ECM proteins.¹³⁻¹⁷ Besides these, some miRNAs have also been noted

*Correspondence to: Ya-ou Zhang and Hsiang-fu Kung; Email: zhangyo@sz.tsinghua.edu.cn and b110473@mailserv.cuhk.edu.hk

Submitted: 12/20/10; Revised: 02/18/11; Accepted: 04/21/11

DOI:

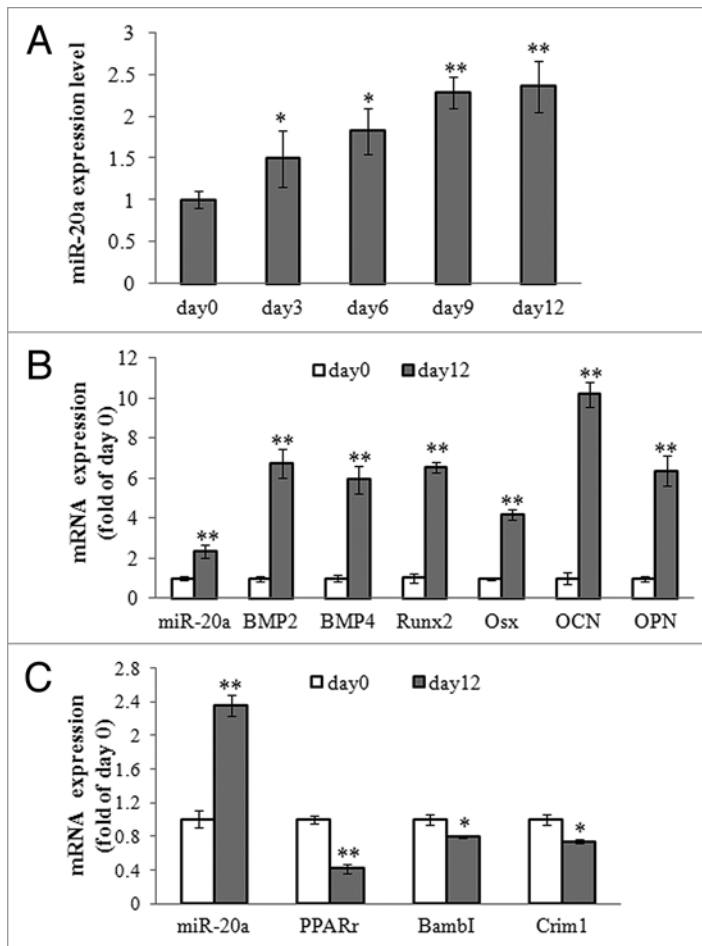


Figure 1. Spatial-temporal expression pattern of miR-20a. Quantitative real-time PCR experiments were carried out to measure the expression levels of miR-20a. (A) Endogenous expression of miR-20a was increased during the osteogenic differentiation of hMSCs. (B) The expression profiles of osteoblast markers and osteogenic regulators. (C) The expression profiles of adipocyte markers and osteoblast inhibitors. * $p < 0.05$ vs. day 0; ** $p < 0.01$ vs. day 0.

to regulate the adipogenesis of preadipocytes. MiR-143 regulates adipocyte differentiation by targeting ERK5; let-7 inhibits clonal expansion and terminates differentiation of 3T3-L1 cells by silencing HMGA2; whereas miR-17-92 promotes adipocyte differentiation by negatively regulating Rb2/p130 in 3T3-L1 cells.¹⁸⁻²⁰

MiR-20a is a member of the miR-17-92 cluster, which is one of the most extensively studied families. The members of this family play important roles in tissue and organ development. Some members of this family (miR17-5p, miR-20a and miR-106a) were found to be involved in monocytic differentiation and maturation.²¹ In addition, the family was also known to be closely associated with tumors,²² autoimmune diseases,²³ as well as osteogenesis.¹⁷ During BMP-2-induced osteogenesis of premyogenic C2C12 cells, it was shown that at least 22 miRNAs (including miR-17-5p, miR-106a and miR-106b) were downregulated in response to BMP-2 signals.¹⁷ However, systemic research on the roles of miR-20a in osteogenic differentiation is still obscure.

In the present study, we discovered a novel role of miR-20a in osteogenic differentiation and dissected its underlying mechanisms in hMSCs.

Results

Spatial-temporal expression pattern of miR-20a. In our preliminary experiment, we found that the level of natural miR-20a was much higher in bone-marrow-derived mesenchymal stem cells (MSCs) derived from young persons (under 20 years) than it was from MSCs derived from adults (30–40 years) (Sup. Fig. 1). To investigate whether and how miR-20a is involved in osteogenic differentiation, BM-MSCs derived from a 36-year-old donor, spindle morphology under microscopy (Sup. Fig. 2A), were used as a cell model. We found that the endogenous miR-20a expression was significantly increased in the course of osteogenic differentiation from day 3 to day 12 (Fig. 1A). Concomitantly, the miRNA levels of osteogenic markers, including BMP2, BMP4, Runx2, Osx, OPN and OCN, were greatly elevated at day 12 (Fig. 1B and $p < 0.05$), thus suggesting that miR-20a may play an important role in osteogenesis. On the contrary, the mRNA level of adipocyte markers PPAR γ and osteoblast inhibitors BamBI and Crim1, was obviously decreased (Fig. 1C and $p < 0.05$). They negatively correlated with the miR-20a expression level.

Promotion of osteogenic differentiation by miR-20a. To investigate the effect of miR-20a on osteogenic differentiation, we transiently transfected hMSCs with fluorescein-labeled miR-20a mimics and their counterpart inhibitor anti-miR20a. As shown in Supplemental Figure 2B, the transfection efficiency was over 90% when viewed 24 hours post-transfection. After quantization by qRT-PCR, we showed that the intracellular miR-20a level in hMSCs transfected with miR-20a mimics was about 8 folds higher than that of those cells transfected with NC or anti-miR20a inhibitor (Fig. 2A). After transfection, hMSCs cells were cultured in a medium supplemented with osteogenic inducers (OS). AKP activity, an early marker of osteogenic differentiation, was assayed at day 6. As shown in Figure 2B, the miR-20a significantly enhanced the AKP activity whereas the anti-miR20a reduced the AKP activity. This indicates that the anti-miR20a functionally inhibited the osteogenesis of hMSCs. We next examined the markers of osteoblast, including Runx2, Osx, OPN and OCN, by qRT-PCR. We showed that the mRNA levels of these markers were significantly increased by miR-20a whereas they were decreased by anti-miR20a (Fig. 2C). Furthermore, we showed that the protein level of Runx2 was significantly increased by miR-20a mimics but that it was decreased by anti-miR20a. However, PPAR γ was largely decreased by miR-20a mimics whereas it was increased by anti-miR20a (Fig. 2D). To further confirm the osteogenic effect of miR-20a, we carried out AKP staining, ARS and Von Kossa staining experiments. We showed that miR-20a stimulated the osteogenic differentiation of hMSCs (Fig. 2E). In contrast, the anti-miR20a suppressed the osteogenic differentiation of hMSCs (Fig. 2).

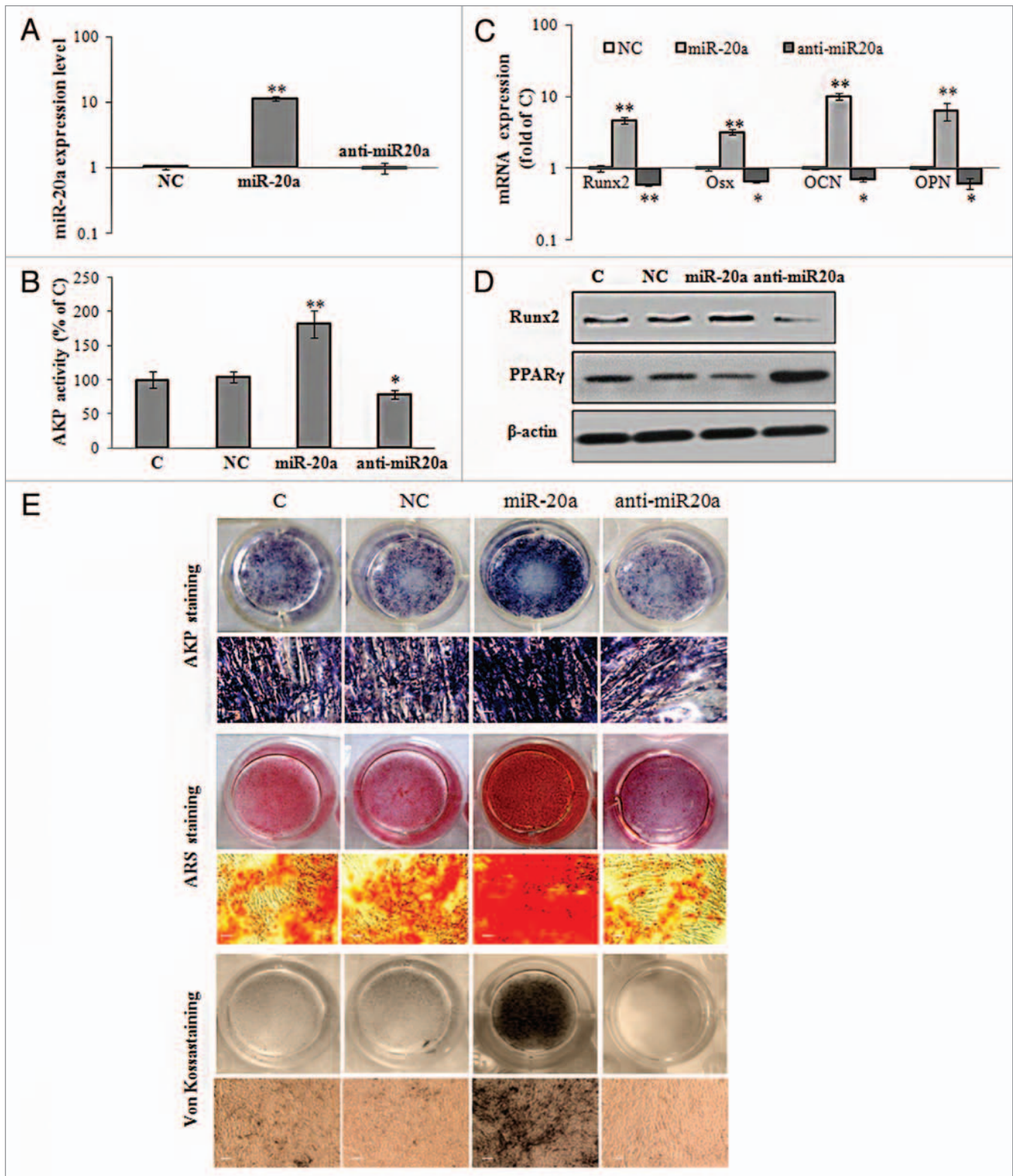


Figure 2. miR-20a promoted osteogenic differentiation of hMSCs. (A) mature miR-20a expression levels after miR-20a mimics or anti-miR20a transfection. (B–D) after transfection, cells were continued to induce osteogenesis by an OS medium. AKP activity was assayed at day 6 (B), mRNA levels of osteogenic markers Runx2, Osx, OPN and OCN were quantified at day 12 (C), and protein levels of Runx2 and PPAR γ were assayed at day 12 (D). (E) Results of cellular staining by AKP (for AKP activity), ARS (for calcium knots) and Von Kossa (for mineralization) at day 12. Scale bar: 25 μ m. C, Non-transfection; NC, negative control transfection; miR-20a, miR-20a mimics transfection; anti-miR20a, anti-miR20a transfection. * $p < 0.05$ Vs. NC; ** $p < 0.01$ Vs. NC.

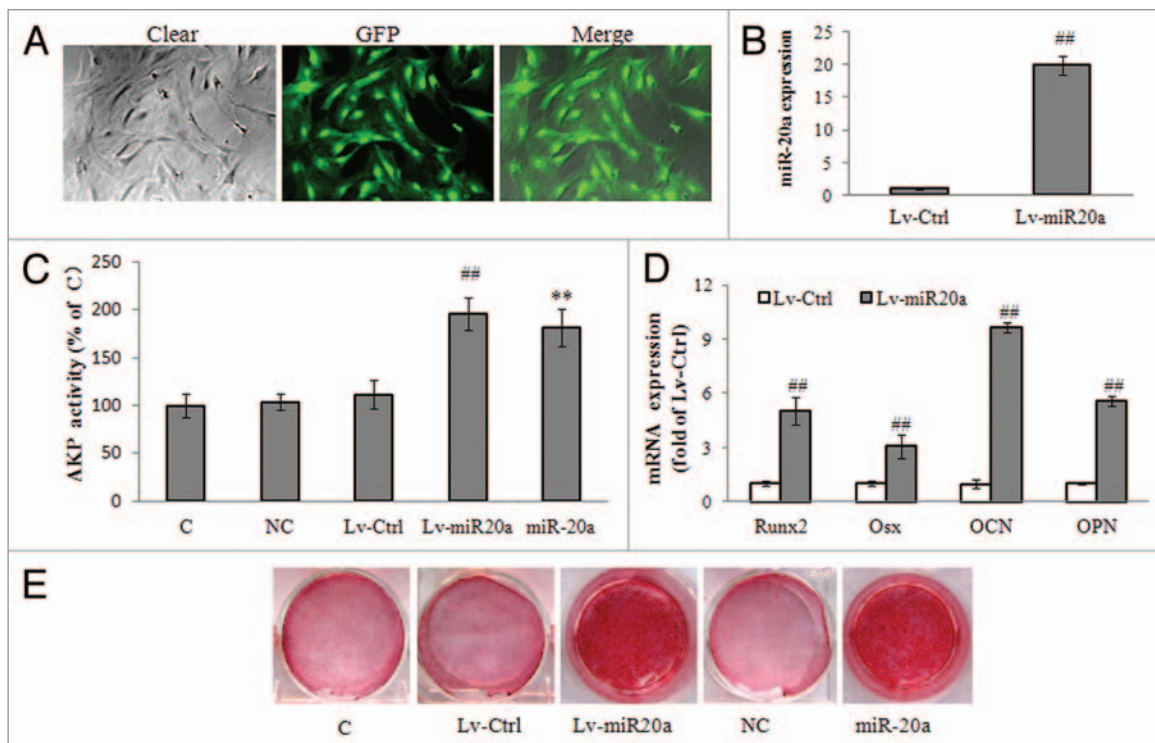


Figure 3. Stable overexpression of miR-20a enhanced osteogenic differentiation of hMSCs. (A) Lv-miR20a infected hMSCs at almost 100% when viewed by EGFP expression. (B) the expression levels of miR-20a after hMSCs were infected with LV-miR20a. (C–E) miR-20a and Lv-miR20a transfected or infected hMSCs and cultured in OS medium. AKP activity was measured at day 6 (C). Expression profiles of bone markers (Runx2, Osx, OPN and OCN) were assayed at day12 (D) and ARS staining was performed at day 12 (E). ***p* < 0.01 Vs. NC; ##*p* < 0.01 Vs. Lv-Ctrl.

Following observation of miR-20a-mimics-mediated osteogenesis, we constructed lentiviral vectors (Lv-miR20a) to stably express miR-20a in the hMSCs. The Lv-miR20a vector infected the hMSCs at almost 100% efficiency (Fig. 3A). After infection, mature miR-20a was stably expressed in the hMSCs (Fig. 3B). The AKP activity induced by the Lv-miR20a infection was similar to that induced by the miR-20a mimics (Fig. 3C). The mRNA level of osteoblast markers, as well as osteogenic regulators Runx2, Osx, OPN and OCN, was also significantly elevated by Lv-miR20a transduction (Fig. 3D). Compared with the controls, much stronger ARS staining was also observed in Lv-miR20a-infected cells (Fig. 3E).

Upregulation of BMP/Runx2 signaling by ectopic miR-20a. It is well known that BMP/Runx2 signaling plays an important role in regulating osteoblast differentiation. To further dissect the molecular mechanism of miR-20a-mediated osteogenesis, we measured the mRNA and protein levels of BMP2, BMP4 and Runx2, the main regulators on the pathway after the overexpression of miR-20a and anti-miR20a mimics. The results from the RT-PCR and enzyme-linked immunosorbent assay (ELISA) experiments showed that both the transcriptional (Fig. 4A) and translational (Fig. 4B) levels of BMP2, BMP4 and Runx2 were significantly elevated by miR-20a but that they were decreased by anti-miR20a.

Upregulation of BMP signaling by miR-20a via targeting PPAR γ . MiR-20a mimics and Lv-miR20a had a similar effect on osteogenic differentiation and we speculated that

miR-20a-mediated osteogenesis possibly occurred at the early stage. By using the bioinformatic approach,²⁴ PPAR γ was predicted to be a target of miR-20a. PPAR γ is a critical activator in adipogenic differentiation but it acts as a negative regulator in osteogenesis. Moreover, PPAR γ decides the cell fate in early differentiation.³ In this study, we found that the PPAR γ expression was suppressed by the miR-20a mimics and the PPAR γ -specific siRNA (PPAR γ -Si) both at the mRNA and protein levels (Fig. 5A). Furthermore, we showed that the markers of osteoblast and the regulators of osteogenesis, including Runx2, Osx, OCN and OPN, were enhanced either by miR-20a or PPAR γ -Si at day 3 and day 6 (Fig. 5B).

To further identify whether PPAR γ is the direct target of miR-20a, we inserted 3'-UTR of PPAR γ with the binding sites or mutated binding sites into the luciferase reporter vector pRL-TK (Fig. 5C) to generate PPAR γ -WT and PPAR γ -Mu vectors. The miR-20a was cotransfected either with PPAR γ -WT or PPAR γ -Mu vector into Cos-7 cells. The luciferase activity was then measured to determine the corresponding effects. Compared to NC, the luciferase activity was reduced by 28% by miR-20a in the case of the PPAR γ -WT sequence. However, the luciferase activity was not affected by a simultaneous transfection with the miR-20a and PPAR γ -Mu vector (Fig. 5D). These results suggested that miR-20a regulated the PPAR γ expression by directly targeting the 3'-UTR of PPAR γ .

To confirm the negative effect of PPAR γ on osteogenic differentiation, we transfected PPAR γ -Si into hMSCs. By using the

ARS staining assay, we demonstrated that osteogenesis was strongly promoted (Fig. 5F). Concomitantly, the expression level of BMP2, BMP4 and Runx2 was significantly upregulated either by the PPAR γ knockdown or by the miR-20a overexpression (Fig. 5E).

Identification of new targets of miR-20a—Bambi and Crim1. By using various bioinformatic softwares, such as the miRanda, Pictar and TargetScan, Bambi and Crim1, the antagonists of BMP signaling pathway, were well recognized as the putative target genes of miR-20a. To confirm whether they were also potential targets of miR-20a, we first checked the expression level of Bambi and Crim1 when miR-20a was overexpressed. Our results showed that both the mRNA and protein levels of Bambi and Crim1 were significantly reduced by miR-20a (Fig. 6A).

To investigate whether miR-20a directly targets Bambi and Crim1, we amplified the 3'-UTR (nt 237 bp) of Bambi and the 3'-UTR (nt 174 bp) of Crim1 by PCR and inserted them into the same luciferase reporter vector as PPAR γ (Fig. 6B). Similarly, reporter vectors with mutated putative target sites were also generated. Compared to NC, the luciferase activity was reduced by 48% and 37%, upon cotransfection of miR-20a with the Bambi-WT vector (Fig. 6C-1) and the Crim1-WT vector (Fig. 6C-2), respectively. On the contrary, no suppressive effect was detected by miR-20a when the putative target sites were mutated (Fig. 6C). Taken together, our results indicated that miR-20a directly targeted the 3'-UTR of both the Bambi and Crim1.

We further investigated the effects that Bambi and Crim1 on osteogenic differentiation. As shown in Figure 6D and E, the silence of Bambi and Crim1 by specific siRNAs (Bambi-Si and Crim1-Si) enhanced the osteogenesis of hMSCs when viewed by the ARS assay. Consistent with the enhanced osteogenic effect, the expression levels of BMPs and Runx2 were also significantly elevated after the knockdown either of Bambi or Crim1. Compared to miR-20a, we noticed that the osteogenic effect of the Crim1 or the Bambi knockdown was weaker than that of the miR-20 overexpression. Our results demonstrated that Bambi and Crim1 acted as negative factors in the osteogenesis of hMSCs.

Co-regulation of osteogenesis by miR-20a via three targets. It is well known that groups of functionally related genes act together to regulate biological significance. A miRNA with the ability to target multiple genes could regulate hundreds of protein-coding genes with a regulatory network.²⁵ In this study, we revealed that miR-20a promoted osteogenic differentiation through co-regulatory pathways. MiR-20a directly targets PPAR γ , Bambi and Crim1, and this leads to the activation of BMP/Runx2 signaling and the promotion of the osteogenesis of hMSCs (Fig. 7).

Discussion

Osteoporosis is a disease of progressive bone loss associated with an increased risk of fractures, and it has become a major health problem in the aging population. Mesenchymal stem cells (MSCs) have been regarded as one of the potential candidates

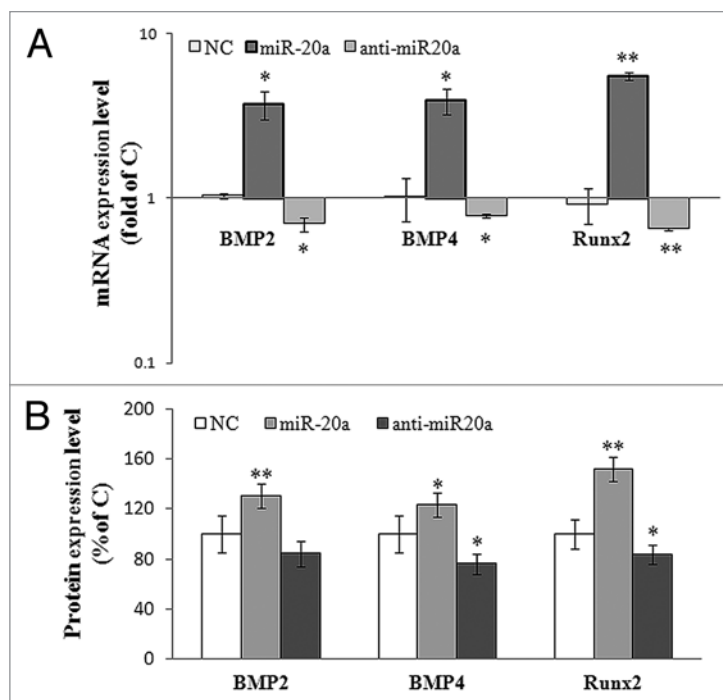


Figure 4. miR-20a upregulated BMP signaling pathway. The mRNA and protein expression level of BMP2, BMP4 and Runx2 were elevated by miR-20a overexpression. (A) Results of qRT-PCR. (B) ELISA analysis. * $p < 0.05$ Vs. NC; ** $p < 0.01$ Vs. NC.

because they can differentiate into osteoblasts which are responsible for bone formation. MiRNAs are known to play key roles in osteoblast differentiation. For example, miR-26a, miR-29b, miR-196 and miR-125b were all involved in osteoblastic differentiation.¹³⁻¹⁶ However, these researches were only confined to the function, whereas systemic research on the regulatory mechanism was obscure. In our study, different miR-20a expression levels were observed in BM-MSCs derived from young persons and adults; in addition, the endogenous miR-20a expression level was elevated during the course of osteogenic differentiation. We therefore speculated that miR-20a possibly stimulated the osteogenesis of hMSCs. Next, we demonstrated the enhancing-osteoblast effect of miR-20a by using biological experiments, and a co-regulatory mechanism was discussed.

In the osteogenesis of MSCs, Runx2 is a crucial factor because it provides a permanent directional signal for lineage determination, whereas BMPs mediate osteogenesis through the activation of transcription factors similar to Runx2.^{2,5} Our data demonstrated that the miR-20a-activated BMPs and Runx2 both at the mRNA and the protein expression levels (Fig. 4A and B). However, their relationship might not be direct because miRNAs frequently modulate gene expression through binding to the 3'-UTR of their target genes, thus leading to translational repression or miRNA degradation.¹¹ Therefore, it is possible that miR-20a upregulated the expression both of BMPs and Runx2 by suppressing their negative regulators or antagonists.

It is well-known that an average miRNA has approximately 100 target sites and that it regulates a large fraction of

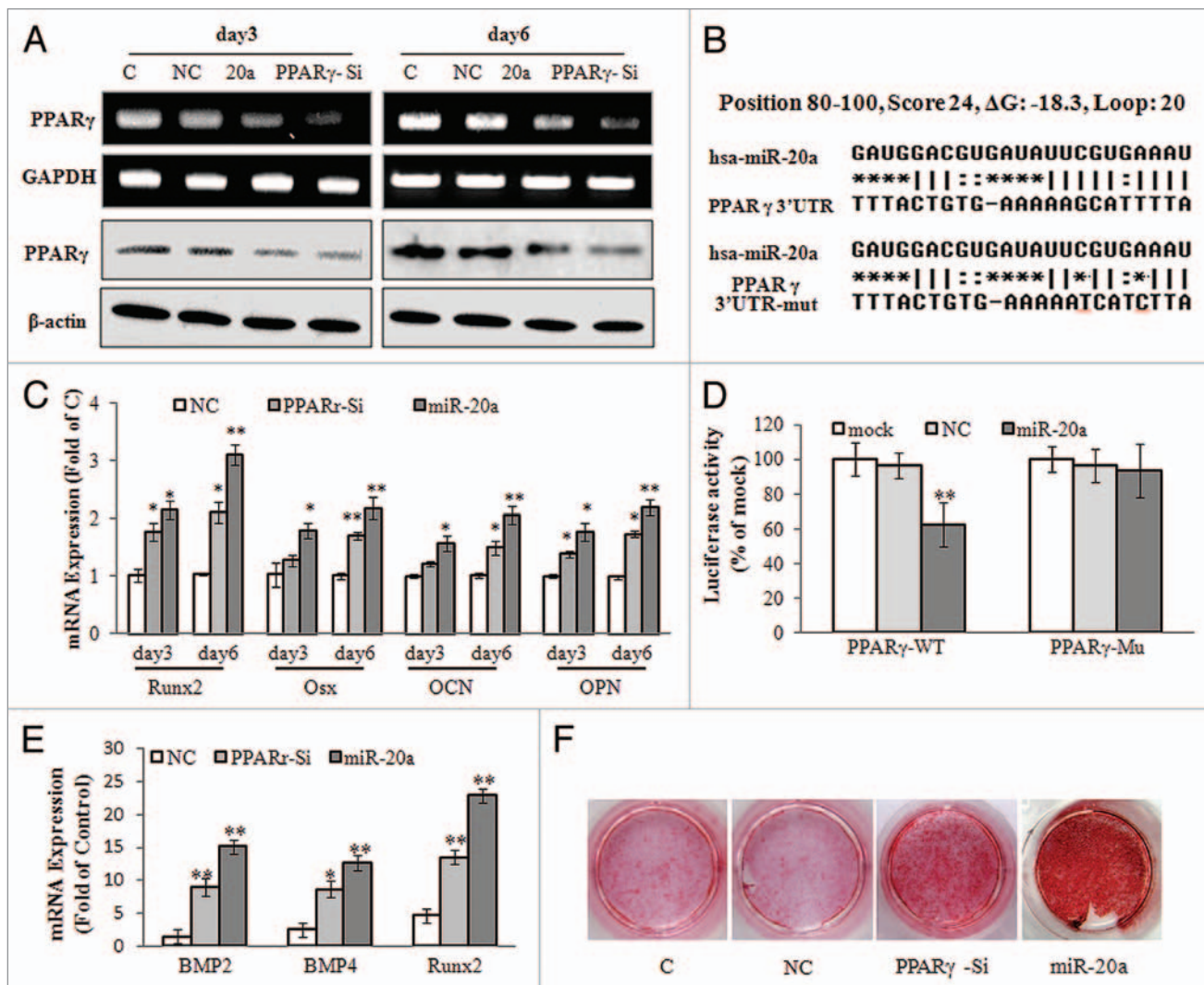


Figure 5. PPAR γ was a target of miR-20a and it suppressed osteogenesis of hMSCs. (A) Expression of PPAR γ was repressed by miR-20a mimics and PPAR γ -specific siRNA (PPAR γ -Si) both at mRNA and Protein level. (B) Expression profiles of osteoblast markers (Runx2, Osx, OPN and OCN) at day 3 and day 6. (C) Diagram of PPAR γ 3'-UTR containing binding sites. (D) Luciferase reporter assays in Cos-7 cells, with co-transfection of wt or mt 3'-UTR and miRNAs as indicated. (E) BMPs and Runx2 expression were stimulated by PPAR γ -Si and miR-20a. (F) ARS staining results of hMSCs transfected with PPAR γ -Si and miR-20a. * $p < 0.05$ Vs. NC; ** $p < 0.01$ Vs. NC.

protein-coding genes, which form a regulatory network.²⁵ In our investigation, PPAR γ was found to be a target gene of miR-20a, which helps us to deduce the association between the osteogenic activity of miR-20a and PPAR γ activation. PPAR γ is one of the most important cell-fate-defining factors in MSCs, and it positively regulates adipogenesis but negatively regulates osteogenesis. The previous study showed that PPAR γ activation inhibited the transcription of Runx2,²⁶ as well as downregulating the BMPs' expression.²⁷ As a transcription factor, PPAR γ is a member of nuclear hormone receptor gene superfamily that regulates ligand-dependent transcriptional activation and repression. It is a well-known major factor in defining adipogenic lineage,³ and it also plays a pleiotropic role in controlling cell homeostasis through cross-talking with other nuclear receptors.²⁸ It is known to be involved in the differentiation of mesenchymal cells into osteoblasts and it also plays an essential role in the maintenance of

bone homeostasis. In an earlier study, an antidiabetic thiazolidinedione drug, Rosiglitazone (Rosi), was found to decrease BMD and bone volume by increasing the PPAR γ activity. This kind of bone loss is believed to be associated with a decreased number of osteoblasts and a lower expression of key osteogenic transcription factors such as Runx2 and Osterix in the cultures of marrow-derived mesenchymal progenitors.^{29,30} Consistent with these results, downregulation of PPAR γ activity was also observed during cases of increasing bone mass and osteoblast number.³¹ In addition, the PPAR γ -repressed osteoblast phenotype was thought to be initiated by a diminished expression of osteoblast-specific signaling pathways, including BMPs and Runx2.²⁷

Antagonists of the BMP signaling pathway are generally categorized at three levels: extracellular (Noggin, Gremlin, Chordin); cell surface (Bambi and Crim1); and intracellular inhibitory (Smads 6 and 7).³² Based on our findings, Bambi and Crim1

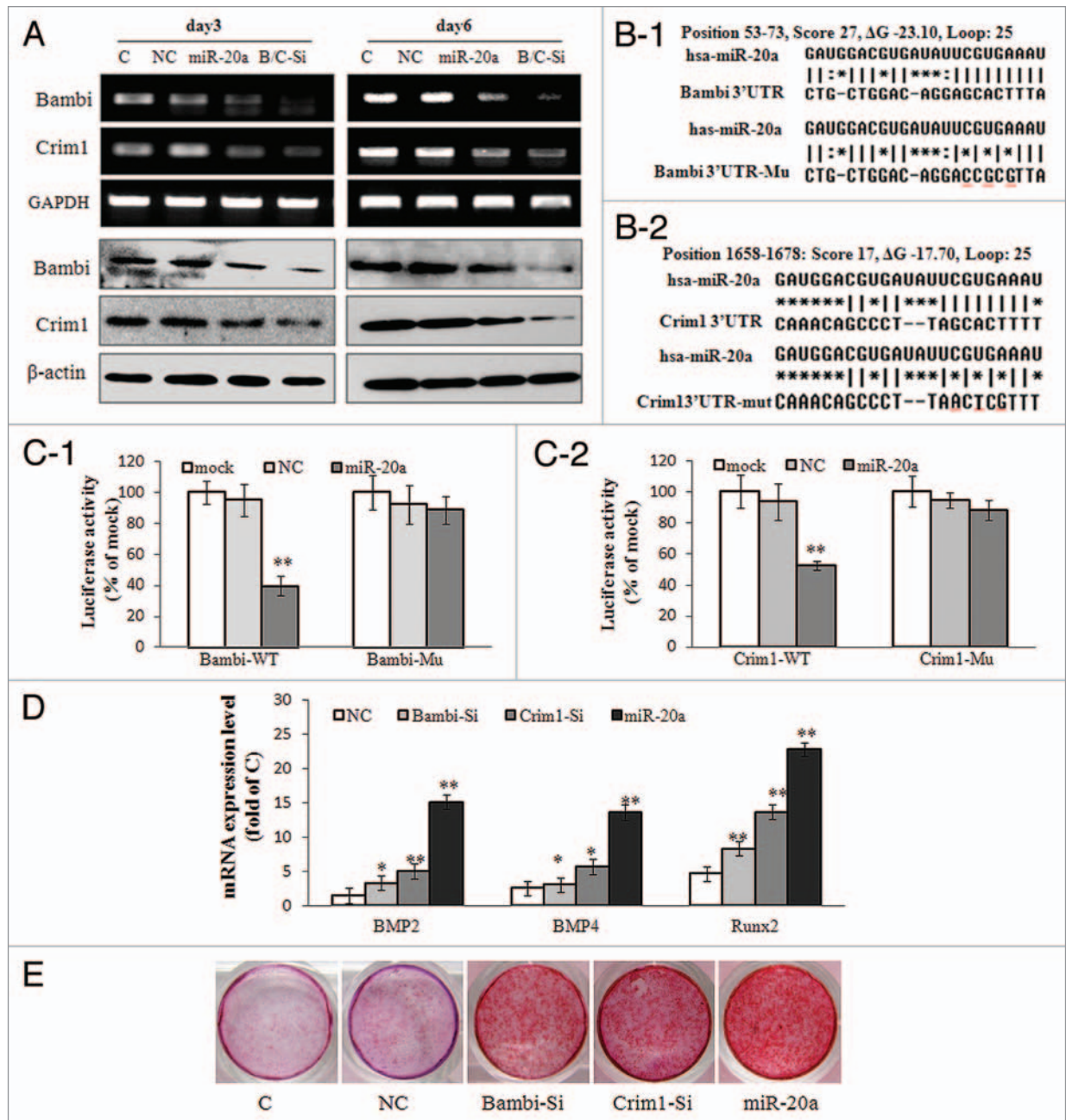


Figure 6. Bambi and Crim1 were novel targets of miR-20a. (A) the expression of Bambi and Crim1 were downregulated by their respective siRNA and miR-20a. (B) Diagram of Bambi (B-1) and Crim1 (B-2) 3'-UTR containing binding sites. (C) Luciferase reporter assays in Cos-7 cells, with co-transfection of wt or mt 3'-UTR and miRNAs. (D) BMPs and Runx2 expression were stimulated by Bambi-Si, Crim1 and miR-20a. (E) ARS staining assay after hMSCs were transfected with Bambi-Si, Crim1-si and miR-20a. * $p < 0.05$ Vs. NC; ** $p < 0.01$ Vs. NC.

possess high score binding sites for miR-20a in their 3'-UTRs, which indicates that they are the potential targets for the miR-20a in the BMP signaling pathway. In fact, Bambi is a pseudo-receptor of the BMP signaling pathway and it is highly similar in its amino acid sequence to that of the TGF β type-I receptors. However, its intracellular domain is short and lacks a serine/threonine-kinase domain that is essential for phosphorylating downstream targets.³² Nevertheless, its ability to associate with BMP ligands and functional BMP receptors still remains, and thus it

could inactivate ligand-receptor complexes and antagonize BMP signaling.³³ The downregulation of Bambi by miR-20a, therefore, might free more BMP molecules for the functional BMP receptors to bind and thereby increase the expression of Runx2. Crim1 is known to play a pivotal role in the tethering of growth factors at the cell surface,³⁴ and it could bind to the BMPs in order to retard their secretion as mature active proteins, and reduce the processing of preprotein to mature BMP, and finally tether these preproteins to the cell surface.³⁵ In this study, the suppression of

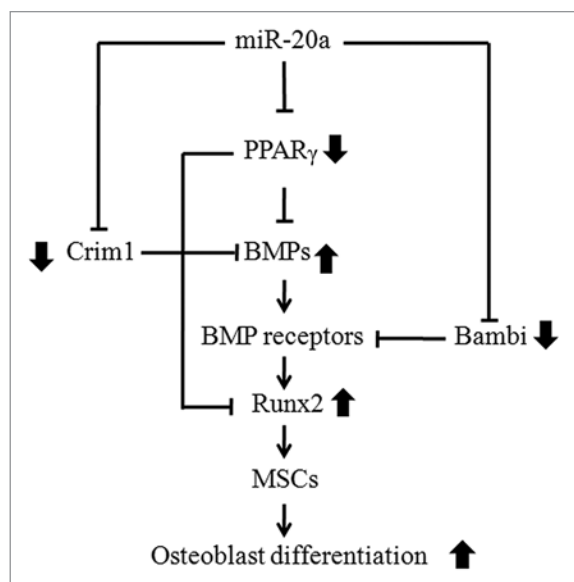


Figure 7. The co-regulatory mechanism of miR-20a in osteoblast differentiation.

Crim1 was observed after the transfection of miR-20a, resulting in an increase of effective BMP concentration in the media, together with affected BMP processing and delivery to the cell surface. It is postulated that such an increase of free, mature and active BMPs may activate BMP signaling, thus enhancing the osteogenesis of MSCs, as was demonstrated in our study.

The co-regulatory principle of miRNAs is not a new concept, and it has been mentioned in many papers.^{12,24} However, it is only speculated by reasoning and few reports have validated it in practice. One miRNA has the ability to target multiple genes and it could potentially regulate a group of functionally related genes.¹² In our study, we determined that miR-20a activated BMP signaling through targeting PPAR γ , Bambi and Crim1, all of which negatively regulated BMP signaling. The individual SiRNA of PPAR γ , Bambi or Crim1 improved osteogenic differentiation and BMP signaling; however, the effect is mild compared to that of miR-20a. MiR-20a induced a powerful effect possibly because of the combination of three mild effects. Therefore, the accumulation of mild regulation from individual target genes could lead to a significant function of miR-20a. We called this regulatory pattern a co-regulatory mechanism (Fig. 7).

In summary, our results suggested that the miR-20a-enhanced osteogenesis of MSCs may be caused by activating BMP/Runx2 signaling. Furthermore, miR-20a co-repressed several genes related to the BMP/Runx2 signaling pathway, including PPAR γ , Bambi and Crim1, to accumulate mild regulation from the individual target gene and finally significantly enhanced the osteogenesis of hMSCs.

Material and Methods

Cell culture and induction of osteogenic and adipogenic differentiation. hMSCs were isolated from bone marrow and identified by cell surface markers.³⁶ Briefly, bone marrow was aspirated

from healthy donors after formal consent and approval by the local ethics committee. hMSCs were cultured in Minimum Essential Medium Alpha Medium (α -MEM) supplemented with 10% FBS, 2 mM L-Glutamine, 100 U/mL penicillin and 100 μ g/mL streptomycin and incubated in a humidified atmosphere of 5% CO₂ at 37°C. After four passages, the surface markers CD3, CD16, CD19, CD33, CD34, CD38, CD133, HLA-DR, CD29, CD44, CD90 and CD166 were assayed.

Osteogenic and adipogenic differentiation of MSCs were induced according to a previously published protocol.³⁶ The OS medium was supplemented with osteogenic inducers: including 10⁻⁸ M dexamethasone (Dex); 50 μ g/mL ascorbic acid 2-phosphate (AsAP); and 10 mM Glycerol 2-phosphate (Gly) (Sigma, USA). For adipogenesis, the OA medium was the α -MEM medium supplemented with 10% FBS, 10⁻⁷ dexamethasone, 50 μ M indomethacin, 10 μ g/ml Insulin and 0.45 mM 3-isobutyl-1-methyl-xanthine (Sigma, USA). hMSCs were seeded at density of 5 \times 10⁵ cells per well in a 12-well plate, and the culture medium was replaced with an OS or OA medium when the cells reached 80% confluence. The cells were then incubated with medium change every three days.

miRNAs and siRNAs transfection. miRNAs and siRNAs were synthesized by Shanghai GenePharma Co., (Shanghai, China). MiR-20a and anti-miR20a were designed according to the miRBase sequence database (<http://microrna.sanger.ac.uk>). The sequence of miR-20a mimics was 5'-GGU AUC UUG AUG UGC CAC GUG AGC UUG-3'. The sequences of target-specific SiRNAs were: PPAR γ , 5'-GAC AUU CCA UUC ACA AGA A-3'; Bambi, 5'-AUC UGA GCU CAG CGC CUG CTT-3'; Crim1, 5'-GCG GGC GUU UGC GAA GAU GTT-3'. Random sequence was used as negative control (NC). hMSCs were seeded into 24 well plates and transfected with siRNA or miRNA duplexes at a concentration of 20–30 pmol/well by using Lipofectaimine 2000 (Invitrogen Corp. Carlsbad, CA, USA) according to the manufacturer's instructions. The medium was replaced 6 hours later whereas the cells were collected 24 hours after transfection for total RNA isolation. Continuous culture was also allowed for the induction of osteogenetic differentiation.

Lentiviral vectors and transduction. To construct a lentiviral vector for miR-20a (110 nt), a DNA fragment encoding pre-microRNA was amplified by PCR from human genomic DNA. The PCR primers were: Forward-5'-CCG GAT ATC TAT CTG ATG TGA CAG CTT CTG-3' and Reverse-5'-CCT TAA TTA AAA GCT GGA GTT CTA CAG CTA G-3'. The PCR product was digested with the restriction enzymes Pac I and EcoR V, and inserted into the Lenti-vector PSMPUW. The correction of the inserted fragment was verified by automated sequencing. A lentiviral vector expressing a scrambled miRNA was used as control. The VSV-G pseudotyped lentivirus was produced by cotransfecting 293LTV cells with the transfer vector and three packaging vectors PCgpV pRSV-REV, and pCMV-VSVG. Subsequent purification was performed by ultracentrifugation. Cells were plated in 24-well plates and transduced with lentiviral vectors and 4–6 μ g/mL polybrene (Sigma, USA).

AKP assay. hMSCs were seeded at a density of 2 \times 10⁵ cells per well in 24-well plates, and were transfected with miRNAs

within 24 hours. Cells were lysed on day 6 and day 9 with a lysis buffer composed of 20 mM Tris-HCl (pH 7.5), 150 mM NaCl and 1% Triton X-100. Intracellular alkaline phosphatase activity was determined by using an AKP activity kit (Nanjing Jiancheng Biotech, China). The protein concentration of cell lysate was determined by using Bradford assay (Bio-Rad, USA) at 595 nm on a microplate spectrophotometer (TECAN, Australia). The specific AKP activity was normalized to the protein concentration. Each experiment was repeated in sextuple.

Mineralization assay: ARS and Von Kossa staining. After MSCs were fixed in 4% paraformaldehyde (m/v) for 10 minutes, samples were evaluated by ARS and Von Kossa staining. Briefly, cells were stained with 2% ARS (pH 4.1) for 15 minutes and then washed twice with deionized water. The orange and red positions were recognized as calcium deposits. For Von Kossa staining, cells were stained with a 1% silver nitrate solution. After 20 minutes of UV exposure, cells were washed with deionized water and placed in 5% sodium thiosulfate for 5 minutes. Cells were then washed three times with deionized water. Black-stained spots were regarded as calcium deposits.

Enzyme-linked immunosorbent assay (ELISA). The protein concentrations of BMP-2, BMP-4 and Runx2 in the cell lysates were determined by using ELISA Kits (R&D system, Minneapolis, MN USA). Briefly, samples were added to the coated wells of 96-well plates and incubated for 1 hour at room temperature. They were washed 3–5 times and incubated with an HRP-linked antibody for 30 minutes at 37°C. The absorbance was measured at 450 nm on the microplate spectrophotometer (TECAN, Austria). All the experiments were repeated in quadruple.

Reverse transcriptase-polymerase chain reaction (RT-PCR). hMSCs were harvested on day 1, day 2 and day 3 after induction with an OS or an OA medium. The total RNA was extracted by using Trizol reagent (Invitrogen, USA) according to the manufacturer's instructions. Reverse transcription was carried out by using SuperScript™ III Reverse Transcriptase (Invitrogen, USA). The cDNA fragments were amplified by using GoTaq® DNA Polymerase (Promega, USA). Thermocycling was performed with a gradient thermocycler (Takara, Japan) which used GoTaq® Flexi DNA Polymerase (Promega, USA). Primers used in the PCR reactions were listed in Supplemental Table 1.

Quantitative real time PCR (qRT-PCR) analyses. miR-20a was analyzed by using the TaqMan microRNA assay kit (Applied Biosystems, USA) and normalized with U6 RNA, which was used as an internal control. qRT-PCR was performed by using

a 7500 Real Time PCR system (Applied Biosystems, USA) with a thermocycler profile at 94°C for 3 minutes, followed by 40 cycles of 94°C, 15 seconds, 62°C, 40 seconds according to the manufacturer's protocol. Fold change was calculated by using the $\Delta\Delta C_t$ method of relative quantification.^{37,38} All experiments were repeated in quadruple.

Western blotting. Cell lysates were separated by SDS-PAGE (12%) and transferred to PVDF membranes. Membranes were blocked with 5% non-fat dry milk for 1 hour and incubated with a monoclonal antibody against Bambi, Crim1 (Abcam, USA), or a rabbit polyclonal antibody against PPAR γ (Boshide Company, China) overnight. After rinsing, the membrane was incubated with a HRP-conjugated secondary antibody (Santa Cruz Biotechnology, CA USA), and detected by chemoluminescence. The β -actin protein was used as an internal loading control.

Luciferase assays. Luciferase assays were performed according to a previously published protocol.¹¹ In brief, the 3'-UTRs of Bambi (nt 14–250), Crim1 (nt 1,584–1,758) and PPAR γ (nt 23–207) and their corresponding mutated 3'-UTR were amplified by PCR by using the primers shown in Table 1. The target sequences were cloned into the pRL-TK reporter vector (Promega, USA). Cos-7 Cells were seeded in 24-well plates at a density of 1×10^5 cell/well. On the next day, a reporter plasmid (300 ng) was co-transfected with a miRNA (at a final concentration of 20 nM) by using Lipofectamine 2000. Cell lysates were collected 30 hours after transfection. Renilla luciferase activities were measured by using a Luciferase Reporter Assay System (Promega, USA). Each experiment was repeated in triplication. The protein concentration of cell lysates was determined at 595 nm by using Bradford assay (Bio-Rad, USA) on a spectrophotometer (TECAN, Australia). The luciferase activity was normalized by the total protein content.

Statistical analysis. Data are expressed as mean \pm SD. Statistical analysis was performed by using the independent samples t-test (SPSS, USA). A p-value of less than 0.05 was considered statistically significant.

Acknowledgments

This project is supported by the National Natural Science Foundation of China (No. 30871428) and Double Hundred Project of Shenzhen.

Note

Supplemental materials can be found at: www.landesbioscience.com/journals/rnabiology/article/16043

References

1. Chamberlain G, Fox J, Ashton B, Middleton J. Concise review: mesenchymal stem cells: their phenotype, differentiation capacity, immunological features and potential for homing. *Stem Cells* 2007; 25:2739-49.
2. DUCY P, ZHANG R, GEOFFROY V, RIDALL AL, KARSENTY G. Osf2/Cbfa1: a transcriptional activator of osteoblast differentiation. *Cell* 1997; 89:747-54.
3. ROSEN ED, WALKER CJ, PUIGSERVER P, SPIEGELMAN BM. Transcriptional regulation of adipogenesis. *Genes Dev* 2000; 14:1293-307.
4. BI W, DENG JM, ZHANG Z, BEHRINGER RR, de Crombrughe B. Sox9 is required for cartilage formation. *Nat Genet* 1999; 22:85-9.
5. PHIMPHILAI M, ZHAO Z, BOULES H, ROCA H, FRANCESCHI RT. BMP signaling is required for RUNX2-dependent induction of the osteoblast phenotype. *J Bone Miner Res* 2006; 21:637-46.
6. YEH WC, CAO Z, CLASSON M, MCKNIGHT SL. Cascade regulation of terminal adipocyte differentiation by three members of the C/EBP family of leucine zipper proteins. *Genes* 1995; 9:168-81.
7. WIGHTMAN B, HA I, RUVKUN G. Posttranscriptional regulation of the heterochronic gene lin-14 by lin-4 mediates temporal pattern formation in *C. elegans*. *Cell* 1993; 75:855-62.
8. NILSEN TW. Mechanisms of microRNA-mediated gene regulation in animal cells. *Trends Genet* 2007; 23:243-9.
9. KARP X, AMBROS V. Developmental biology. Encouraging miRNAs in cell fate signaling. *Science* 2005; 310:1288-9.
10. XU P, GUO M, HAY BA. MicroRNAs and the regulation of cell death. *Trends Genet* 2004; 20:617-24.
11. AMBROS V. The functions of animal microRNAs. *Nature* 2004; 431:350-5.

12. Hua Z, Lv Q, Ye W, Wong CK, Cai G, Gu D, et al. MiRNA-Directed Regulation of VEGF and Other Angiogenic Factors under Hypoxia. *PLoS One* 2006; 1:116.
13. Luzi E, Marini F, Sala SC, Tognarini I, Galli G, Brandi ML. Osteogenic differentiation of human adipose tissue-derived stem cells is modulated by the miR-26a targeting of the SMAD1 transcription factor. *J Bone Miner Res* 2008; 23:287-9.
14. Li Z, Hassan MQ, Jafferji M, Garzon R, Croce CM, van Wijnen AJ, et al. Biological Functions of miR-29b Contribute to Positive Regulation of Osteoblast Differentiation. *J Biol Chem* 2009; 284:15676-84.
15. Kim YJ, Bae SW, Yu SS, Bae YC, Jung JS. miR-196a Regulates Proliferation and Osteogenic Differentiation in Mesenchymal Stem Cells Derived from Human Adipose Tissue. *J Bone Miner Res* 2009; 24:816-25.
16. Mizuno Y, Yagi K, Tokuzawa Y, Kanesaki-Yatsuka Y, Suda T, Katagiri T, et al. miR-125b inhibits osteoblastic differentiation by downregulation of cell proliferation. *Biochem Biophys Res Commun* 2008; 368:267-72.
17. Li Z, Hassan MQ, Volinia S, van Wijnen AJ, Stein JL, Croce CM, et al. A microRNA signature for a BMP2-induced osteoblast lineage commitment program. *Proc Natl Acad Sci USA* 2008; 105:13906-11.
18. Esau C, Kang X, Peralta E, Hanson E, Marcusson EG, Ravichandran LV, et al. MicroRNA-143 regulates adipocyte differentiation. *J Biol Chem* 2004; 279:52361-5.
19. Sun T, Fu M, Bookout AL, Kliewer SA, Mangelsdorf DJ. MicroRNA let-7 Regulates 3T3-L1 Adipogenesis. *Mol Endocrinol* 2009; 23:925-31.
20. Wang Q, Li YC, Wang J, Kong J, Qi Y, Quigg RJ, et al. miR-17-92 cluster accelerates adipocyte differentiation by negatively regulating tumor-suppressor Rb2/p130. *Proc Natl Acad Sci USA* 2008; 105:2889-94.
21. Fontana L, Pelosi E, Greco P, Racanicchi S, Testa U, Liuzzi F, et al. MicroRNAs 17-5p-20a-106a control monocytopoiesis through AML1 targeting and M-CSF receptor upregulation. *Nat Cell Biol* 2007; 9:775-87.
22. Hayashita Y, Osada H, Tatematsu Y, Yamada H, Yanagisawa K, Tomida S, et al. A polycistronic microRNA cluster, miR-17-92, is overexpressed in human lung cancers and enhances cell proliferation. *Cancer Res* 2005; 65:9628-32.
23. Xiao C, Srinivasan L, Calado DP, Patterson HC, Zhang B, Wang J, et al. Lymphoproliferative disease and autoimmunity in mice with increased miR-17-92 expression in lymphocytes. *Nat Immunol* 2008; 9:405-14.
24. Ye WB, Lv Q, Wong CK, Hu S, Fu C, Hua Z, et al. The Effect of Central Loops in miRNA: MRE Duplexes on the Efficiency of miRNA-Mediated Gene Regulation. *PLoS one* 2007; 3:1719.
25. Brennecke J, Stark A, Russell RB, Cohen SM. Principles of microRNA-target recognition. *PLoS Biol* 2005; 3:85.
26. Jeon MJ, Kim JA, Kwon SH, Kim SW, Park KS, Park SW, et al. Activation of peroxisome proliferator-activated receptor-gamma inhibits the Runx2-mediated transcription of osteocalcin in osteoblasts. *J Biol Chem* 2003; 278:23270-7.
27. Lian JB, Stein GS, Javed A, van Wijnen AJ, Stein JL, Montecino M, et al. Networks and hubs for the transcriptional control of osteoblastogenesis. *Rev Endocr Metab Disord* 2006; 7:1-16.
28. Shockley KR, Lazarenko OP, Czernik PJ, Rosen CJ, Churchill GA, Lecka-Czernik B. PPARgamma2 nuclear receptor controls multiple regulatory pathways of osteoblast differentiation from marrow mesenchymal stem cells. *J Cell Biochem* 2009; 106:232-46.
29. Ali AA, Weinstein RS, Stewart SA, Parfitt AM, Manolagas SC, Jilka RL. Rosiglitazone causes bone loss in mice by suppressing osteoblast differentiation and bone formation. *Endocrinology* 2005; 146:1226-35.
30. Soroceanu MA, Miao D, Bai XY, Su H, Goltzman D, Karaplis AC. Rosiglitazone impacts negatively on bone by promoting osteoblast/osteocyte apoptosis. *J Endocrinol* 2004; 183:203-16.
31. Gimble JM, Zvonic S, Floyd ZE, Kassem M, Nuttall ME. Playing with bone and fat. *J Cell Biochem* 2006; 98:251-66.
32. Gazzero E, Canalis E. Bone morphogenetic proteins and their antagonists. *Rev Endocr Metab Disord* 2006; 7:51-65.
33. Chen J, Bush JO, Ovitt CE, Lan Y, Jiang R. The TGF beta pseudoreceptor gene *Bambi* is dispensable for mouse embryonic development and postnatal survival. *Genesis* 2007; 45:482-6.
34. Pennisi DJ, Wilkinson L, Kolle G, Sohaskey ML, Gillinder K, Piper MJ, et al. *Crim1* mice display a disruption of the *crim1* gene resulting in perinatal lethality with defects in multiple organ systems. *Dev Dyn* 2007; 236:502-11.
35. Wilkinson L, Kolle G, Wen D, Ruta LA, Pennisi D, Kett M, et al. *CRIM1* Regulates the Rate of Processing and Delivery of Bone Morphogenetic Proteins to the Cell Surface. *J Biol Chem* 2003; 278:34181-8.
36. Li G, Zhang XA, Wang H, Wang X, Meng CL, Chan CY, et al. Comparative proteomic analysis of mesenchymal stem cells derived from human bone marrow, umbilical cord and placenta: implication in the migration. *Proteomics* 2009; 9:20-30.
37. Chen C, Ridzon DA, Broomer AJ, Zhou Z, Lee DH, Nguyen JT, et al. Real-time quantification of microRNAs by stem-loop RT-PCR. *Nucleic Acids Res* 2005; 33:179.
38. Lu J, He ML, Wang L, Chen Y, Liu X, Dong Q, et al. MiR-26a inhibits cell growth and tumorigenesis of nasopharyngeal carcinoma through repression of *EZH2*. *Cancer Res* 2011; 71:225-33.